Molecular Crystals and Liquid Crystals Incorporating Nonlinear Optics
Publication details, including instructions for authors and subscription information:
http://www.tandfonline.com/loi/gmcl17

Synthesis, Structure and Properties of $(BEDT\text{-}TTF)_4Hg_3I_8$, a New Organic Bis(ethylenedithio)tetrathiafulvalene-Based Conductor with an Octaiodinemercurate Anion

T. G. Takhirov [a], O. N. Krasochka [a], O. A. Dyachenko [a], L. O. Atovmyan [a], M. Z. Aldoshina [a], L. M. Goldenberg [a], R. N. Lyubovskaya [a], V. A. Merzhanov [a] & R. B. Lyubovskii [a]
[a] The Institute of Chemical Physics of the USSR Academy of Sciences, Chernogolovka, 142 432, USSR
Version of record first published: 22 Sep 2006.

To cite this article: T. G. Takhirov , O. N. Krasochka , O. A. Dyachenko , L. O. Atovmyan , M. Z. Aldoshina , L. M. Goldenberg , R. N. Lyubovskaya , V. A. Merzhanov & R. B. Lyubovskii (1990): Synthesis, Structure and Properties of $(BEDT\text{-}TTF)_4Hg_3I_8$, a New Organic Bis(ethylenedithio)tetrathiafulvalene-Based Conductor with an Octaiodinemercurate Anion, Molecular Crystals and Liquid Crystals Incorporating Nonlinear Optics, 185:1, 215-226

To link to this article: http://dx.doi.org/10.1080/00268949008038504

Mol. Cryst. Liq. Cryst., 1990, Vol. 185, pp. 215–226
Reprints available directly from the publisher
Photocopying permitted by license only

Printed in the United States of America

Synthesis, Structure and Properties of $(BEDT\text{-}TTF)_4Hg_3I_8$, a New Organic Bis(ethylenedithio)tetrathiafulvalene-Based Conductor with an Octaiodinemercurate Anion

T. G. TAKHIROV, O. N. KRASOCHKA, O. A. DYACHENKO, L. O. ATOVMYAN, M. Z. ALDOSHINA, L. M. GOLDENBERG, R. N. LYUBOVSKAYA*, V. A. MERZHANOV, and R. B. LYUBOVSKII

The Institute of Chemical Physics of the USSR Academy of Sciences, Chernogolovka, 142 432 USSR

(*Received October 20, 1989; in final form February 26, 1990*)

The structure of a new organic conductor, $(BEDT\text{-}TTF)_4Hg_3I_8$, has been solved, temperature dependences on conductivity, thermopower and magnetic susceptibility studied. The BEDT-TTF molecules form two different types of stacks. At 260 K a jump in a conductor and thermopower takes place, characterized by a hysteresis of ca. 8 K. At this temperature the phase transition of the first order occurs in $(BEDT\text{-}TTF)_4Hg_3I_8$. Below and above the transition temperature the conductivity has an activation character. At a pressure of 29 kbar the conductivity remains metallic up to 50 K. The paramagnetic susceptibility in this temperature range has a maximum.

Compounds with linear anions are the most thoroughly studied ones among a large number of ion-radical salts based on bis-(ethylenedithio)tetrathiafulvalene (BEDT-TTF) obtained recently. Organic superconductors with linear halide anions I_3^-,[1,2] IBr_2^-[3] and metal halide anions AuI_2^-[4] were obtained in this series. $T_c \sim 10$ K, the maximum value for organic superconductors, was found for a compound with a $[Cu(SCN)_2]^-$ anion.[5] The $(BEDT\text{-}TTF)_4ReO_4$ compound with a tetrahedral anion was also found to be a superconductor with $T_c = 2$ K at $P = 7$ kbar.[6] Thus chain or polymer metal-containing anions are supposed to be able to form structures with a BEDT-TTF molecule undergoing superconductive transition.

Chemistry of mercury salts gives vast possibilities to produce halide-mercurate anions of various structures, among them polymeric.[7,8]

We have succeeded in obtaining at least three phases in each case when synthesizing ion-radical salts of BEDT-TTF with chlorinemercurate, brominemercurate and iodinemercurate anions.

When studying the compounds of the $(BEDT\text{-}TTF)_4Hg_{3-\delta}X_8$ composition, the

superconductive transition was shown to take place at T_c = 1.8 K, P = 12 kbar for $(BEDT\text{-}TTF)_4Hg_{3-\delta}Cl_8$ (X = Cl).[9] $(BEDT\text{-}TTF)_4Hg_{2.89}Br_8$ became superconductive at T_c = 4.3 K at ambient pressure.[10]

The present paper reports on synthesis, crystal structure, and physical properties of the new organic conductor $(BEDT\text{-}TTF)_4Hg_3I_8$ (δ = 0).

EXPERIMENTAL

The $(BEDT\text{-}TTF)_4Hg_3I_8$ crystals were obtained by electrochemical oxidation of BEDT-TTF in tetrahydrofurane under constant current (I = 2 μA) in the presence of electrolyte $(Bu_4N)_2Hg_3I_8$ (obtained by the technique from Reference 11).

Crystallographic data for $(C_{10}H_8S_8)_4Hg_3I_8$: M = 3155.6, a = 11.989(4), b = 8.430(3), c = 40.740(5) Å, γ = 111.08(2)°, V = 3842(2) Å^3, Z = 2, d_{calc} = 2.74 g/cm^3, space group I2/a. The intensities of 927 independent non-zero ($I \geq 36$ (I)) reflections from the 0.2 × 0.3 × 0.1 mm^3 crystal were measured with an automatic four-circle diffractometer RED-4, MoKα-radiation, graphite monochromator, angle interval $0.025 \leq \text{Sin}\,\theta/\lambda \leq 0.450$ Å^{-1}, ω − ω/2ω-technique. Absorption ignored, μ(MoKα) = 102.2 cm^{-1}. The structure was solved by direct methods and refined by least squares by using 889 reflections in full-matrix anisotropic approximation by the Cruickshank weighting scheme. According to the complex program "Reuntgen-75".[12] H atoms were not located. The positions of H atoms were not calculated either, those were only non-hydrogen atoms used in the refinement. Hg atoms were statistically disordered in two positions with the same population of μ = 0.5. The final value R = 0.076. Fractional coordinates and equivalent isotropic temperature factors with e.s.d.'s in parenthesis are given in Table I. Bond lengths and valency angles in the $(BEDT\text{-}TTF)_4Hg_3I_8$ molecule are shown in Table II. The energy of intermolecular interactions (IMIE) of the $BEDT\text{-}TTF^{1/2+}$ cation-radicals was calculated in atom-atom approximation taking into account the "6-exp" potentials by the program given in Reference 13.

DISCUSSION OF THE RESULTS

The crystal structure of $(BEDT\text{-}TTF)_4Hg_3I_8$ is a packing of two crystallographically independent cation-radicals of BEDT-TTF marked as A and B and iodinemercurate anions $Hg_3I_8^{2-}$ (Figure 1). A and B cations have C_2 crystallographic symmetry. Bis(dithio)-tetrathiafulvalene fragments of the A and B cations are plane with the accuracy of ±0.02 and ±0.08 Å, respectively. The deviation of C(1) and C(6) atoms from this average-square plane of A cation are 0.32 and 0.39 Å. Therefore the ethylene groups C(1)-C(1′) and C(6)-C(6′) of the A cation have eclipsed conformation. In the B cation the centers of thermal vibration ellipsoides of C(7) and C(12) atoms are in the plane of the molecule, but large values of respective B_{iso}^{equiv} (Table I) allow to suggest these atoms to have some positional statistical disorder.

Average values of bond lengths in the TTF-fragments of the A and B cations,

TABLE I

Fractional Coordinates and Equivalent Isotropic Temperature Factors
($B_{eq} = 4/3(B_{11}a^2 + B_{22}b^2 + B_{33}c^2 + B_{12}abCos\gamma + B_{13}acCos\beta + B_{23}bcCos\alpha)$

Atom	x	y	z	B_{eq}(Å^2)
I(1)	0,4217(2)	0,4505(3)	0,7275(1)	5,41
I(2)	0,3035(2)	0,7074(3)	0,8044(1)	5,73
Hg(1)	0,5	0,75	0,7422(1)	5,28
Hg(2)	0,3435(3)	0,7507(4)	0,7429(1)	6,70
S(1)	0,1445(6)	0,9051(9)	0,8894(2)	3,06
S(2)	0,1193(6)	0,8820(9)	0,9616(2)	3,45
S(3)	0,1187(6)	0,8826(9)	1,0408(2)	3,18
S(4)	0,1449(6)	0,9070(8)	1,1125(2)	2,80
S(5)	0,3538(7)	1,2475(12)	0,8487(2)	4,74
S(6)	0,3780(6)	1,2517(9)	0,9211(2)	2,81
S(8)	0,3817(6)	1,2615(10)	1,0002(2)	3,38
S(8)	0,3595(7)	1,2681(10)	1,0721(2)	3,99
C(1)	0,0593(24)	0,7730(44)	0,8548(6)	5,24
C(2)	0,0536(22)	0,8066(30)	0,9231(6)	2,59
C(3)	0	0,75	0,9833(8)	2,57
C(4)	0	0,75	1,0187(9)	2,61
C(5)	0,0509(22)	0,8056(32)	1,0777(7)	3,31
C(6)	0,0654(21)	0,7710(35)	1,1461(6)	3,28
C(7)	0,4461(30)	1,2468(77)	0,8141(8)	11,46
C(8)	0,4459(24)	1,2539(34)	0,8826(6)	3,03
C(9)	0,5	1,25	0,9436(12)	5,07
C(10)	0,5	1,25	0,9771(10)	2,55
C(11)	0,4467(21)	1,2536(30)	1,0386(6)	2,11
C(12)	0,4476(28)	1,2567(60)	1,1068(9)	8,00

Angle	ω,°	Angle	ω,°
	Cation A		
C(1)S(1)C(2)	101(1)	S(2)C(3)C(4)	121(1)
C(2)S(2)C(3)	94(1)	S(2′)C(3)C(4)	121(1)
C(4)S(3)C(5)	93(1)	S(3)C(4)S(3′)	117(1)
C(5)S(4)C(6)	101(1)	S(3)C(4)C(3)	122(1)
S(1)C(1)C(1′)	118(1)	S(3′)C(4)C(3)	122(1)
S(1)C(2)S(2)	114(1)	S(3)C(5)S(4)	112(1)
S(1)C(2)C(2′)	129(1)	S(3)C(5)C(5′)	119(1)
S(2)C(2)C(2′)	118(1)	S(4)C(5)C(5′)	129(1)
S(2)C(3)S(2′)	118(1)	S(4)C(6)C(6′)	115(1)
C(7)S(5)C(8)	104(2)	S(6)C(9)C(10)	122(2)
C(8)S(6)C(9)	95(2)	S(6′)C(9)C(10)	122(2)
C(10)S(7)C(11)	96(1)	S(7)C(10)S(7′)	114(1)
C(11)S(8)C(12)	103(2)	S(7)C(10)C(9)	123(2)
S(5)C(7)C(7′)	128(2)	S(7′)C(10)C(9)	123(2)
S(5)C(8)S(6)	115(1)	S(7)C(11)S(8)	114(1)
S(5)C(8)C(8′)	128(2)	S(7)C(11)C(11′)	117(2)
S(6)C(8)C(8′)	117(2)	S(8)C(11)C(11′)	129(2)
S(6)C(9)S(6′)	116(1)	S(8)C(12)C(12′)	128(2)
I(1)Hg(1)I(1‴)	151,5(2)	I(1′)Hg(2′)I(2′)	111,6(2)
I(1)Hg(1)I(2)	94,6(2)	I(1″)Hg(2′)I(2)	100.4(2)
I(1)Hg(1)I(2″)	106,8(2)	I(1″)Hg(2′)I(2′)	101,1(2)
I(2)Hg(1)I(2″)	79,1(2)	I(1″)Hg(2′)I(2′)	112,6(2)
I(1′)Hg(2′)I(1″)	99,9(2)	I(2)Hg(2′)I(2′)	128,1(2)

Symmetry codes:
*Cation A: C(1′), C(2′), C(5′) and C(6′) are x, 3/2 − y, z′.
Cation B: C(7′), C(8′), C(11′) and C(12′) are 1 − x, 5/2 − 7y, z.
Anion: Hg(2′) and T(2′): 1/2 − x, 3/2 − y, 3/2 − z; T(1‴) and T(2″) 1 − x, 3/2 − y, z.

TABLE II

Bond Lengths and Valency Angles in the A, B Cations and the $Hg_3I_8^{2-}$

Bond	d, Å	Bond	d, Å
	Cation A		
S(1)—C(1)	1,86(3)	S(4)—C(6)	1,82(2)
S(1)—C(2)	1,77(2)	C(1)—C(1′)*	1,33(5)
S(2)—C(2)	1,77(2)	C(2)—C(2′)*	1,30(5)
S(2)—C(3)	1,71(2)	C(3)—C(4)	1,44(5)
S(3)—C(4)	1,72(2)	C(5)—C(5′)*	1,24(5)
S(3)—C(5)	1,72(3)	C(6)—C(6′)*	1,48(5)
S(4)—C(5)	1,82(3)		
	Cation B		
S(5)—C(7)	1,79(4)	S(8)—C(12)	1,79(4)
S(5)—C(8)	1,76(3)	C(7)—C(7′)*	1,27
S(6)—C(8)	1,76(3)	C(8)—C(8′)*	1,32(5)
S(6)—C(9)	1,73(3)	C(9)—C(10)	1,36(5)
S(7)—C(10)	1,74(2)	C(11)—C(11′)*	1,30(5)
S(7)—C(11)	1,76(2)	C(12)—C(12′)*	1,30(5)
S(8)—C(11)	1,75(3)		
	Anion $Hg_3I_8^{2-}$		
Hg(1)—I(1)	2,431(2)	Hg(2′)—1(2′)*	2,552(3)
Hg(1)—I(2)	3,391(3)	Hg(2′)—I(1′)*	3,064(3)
Hg(2′)—I(2)	2,720(3)	Hg(2′)—I(1″)*	3,092(3)

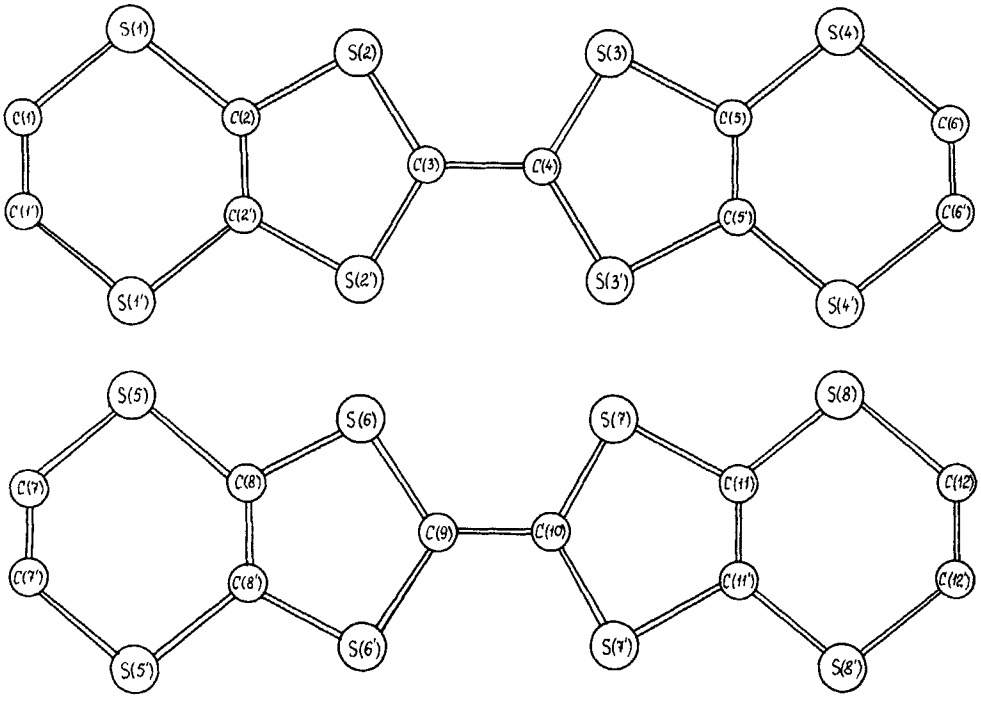

FIGURE to Table II A labeled figure of the asymmetric unit.

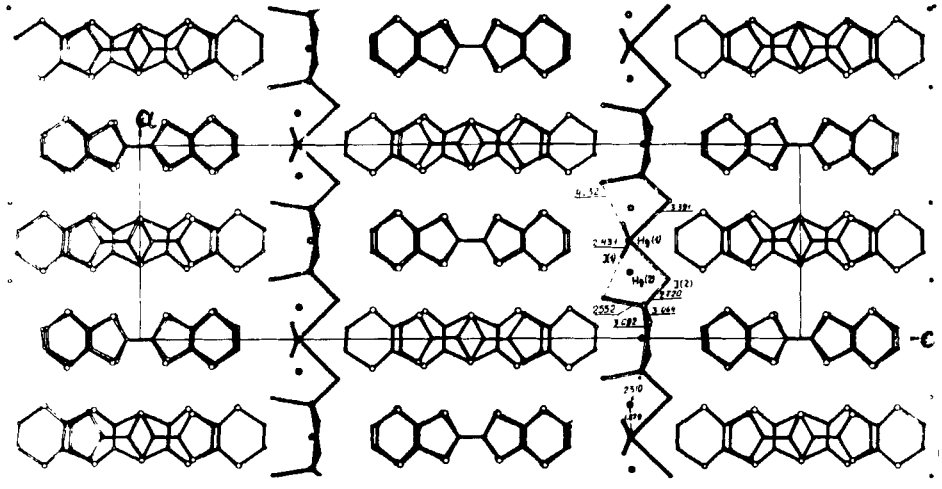

FIGURE 1 Projection of the structure on the ac plane.

in the neutral BEDT-TTF molecule, in the cations with +(1/2) and +1 charge and in the dication of related salts are given in Table III. Comparison of analogous values shows that bond lengths distribution in the B cation corresponds to the charge transfer equal to +(1/2). It leads to the conclusion, that formal charge of the A cation is also equal to +(1/2), although experimental bond lengths do not confirm this suggestion so convincingly as in the case of the B cation.

Cation-radicals and anions form organic and inorganic sheets, respectively, parallel to the **ab** plane and alternating along **c** axis. In organic sheets the ABAB. . . cationic succession forms "corrugated" bands stretching along[110] diagonal (Figure 2), where the A and B molecules tilt to each other at an angle of 46.7°. In each band the neighboring cations A and B are arranged in side-by-side mode and are interconnected by shortened intermolecular contacts of S. . .S type: S(1). . .S(5)

TABLE III

Average Bond Lengths (Å) in the TTF-fragment of BEDT-TTF with the Charge δ Equal to

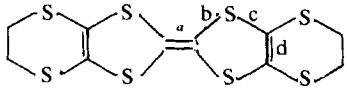

0, +1/2, +1 and +2

δ	a	b	c	d	Reference
0	1,319(1)	1,757(7)	1,754(8)	1,332(7)	14
+1/2	1,365(4)	1,740(2)	1,763(2)	1,329(3)	14
+1	1,38(3)	1,72(1)	1,73(1)	1,37(2)	14
+2	1,455	1,675	1,708	1,374	15
A	1,44(5)	1,72(2)	1,75(3)	1,27(5)	This work
B	1,36(5)	1,74(2)	1,76(3)	1,31(5)	This work

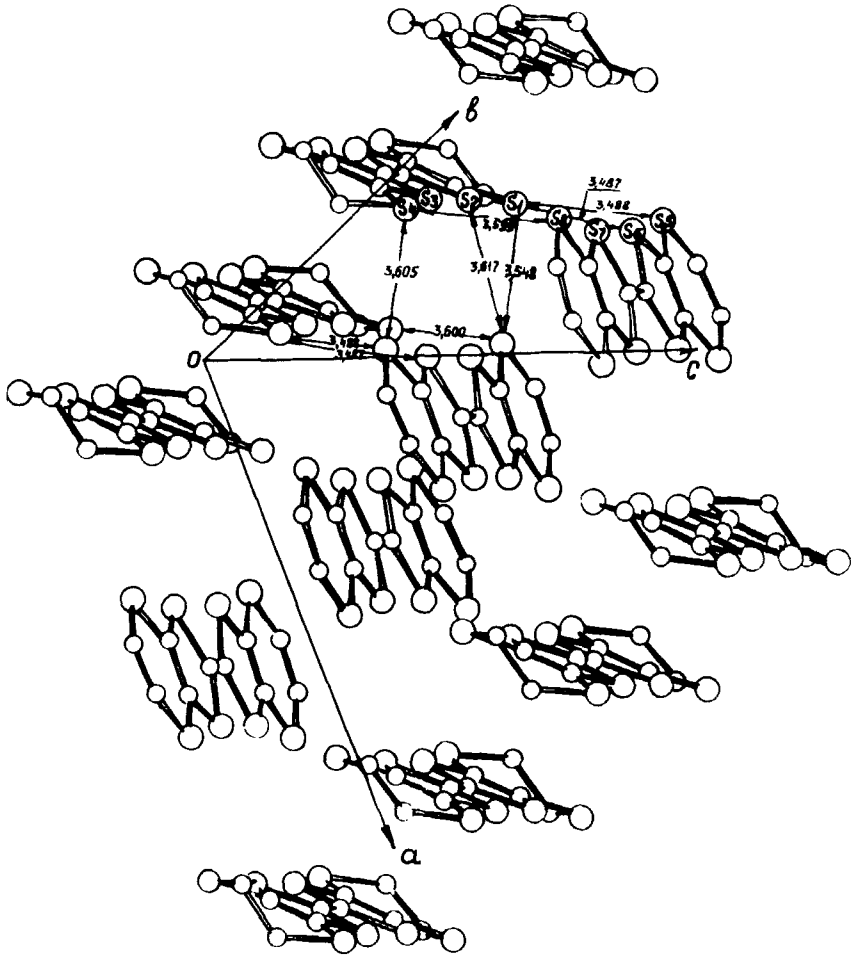

FIGURE 2 The packing of the cationic sheet of the $(BEDT\text{-}TTF)_4Hg_3I_8$ molecules in the crystals.

3.488(9) Å, S(1). . .S(6) 3.487(9) Å, and S(4). . .S(8) 3.599(8) Å. Intermolecular contacts S. . .S have two-dimensional structure because such contacts are observed also between the A and B′ cations from neighboring bands. However, according to the values S(1). . .S(8′) 3.548(9) Å, S(2). . .S(8′) 3.617(8) Å, and S(4). . .S(5′) – 3.605 (9) Å, these interband S. . .S interactions are weaker than intraband ones. Nevertheless, IMIE of the A and B′ cations is somewhat higher than for the A and B cations being −6.40 and 6.19 kcal/mole, respectively. Evidently, it is explained by the fact that IMIE in the $(BEDT\text{-}TTF)_4Hg_3I_8$ structure is determined not by the shortened S. . .S contacts only, but depends on the interaction of other atoms also, which is more essential in the A-B′ pair than in the A-B one.

A succession of cations AAA. . . and BBB. . . is arranged in the stacks of two types, those of A and B parallel to the **b** axis and alternating along the **a** axis (Figure 1). The shortened S. . .S contacts are lacking in the A and B stacks, the

interplanar distances between the cations reaching 3.68 Å (A) and 3.88 Å (B). The stacks A and B are notable for their mode of cation packing: the A cations are fully eclipsed with each other, the B molecules being located zig-zag-wise with a displacement of ca. 3 Å along the cation axis.

The anionic sheets in the $(BEDT\text{-}TTF)_4Hg_3I_8$ structure consist of Hg and I atoms. I atoms are located in such a way that form slightly distorted tetrahedra I_4 with side length lying in the range of 4.327(1)–4.785(1) Å. All I_4 tetrahedra share common apices, edges, and faces forming an infinite zig-zag chain stretching along **a** axis. Inside every I_4 tetrahedron a maximum of electron density is observed which is identified as Hg atom with positional population of 0.5. Partial population of Hg positions and also too short distances between Hg atoms of neighboring tetrahedra (Hg(1). . .Hg(2) 1.879(3) Å, Hg(2). . .Hg(2′) (1/2 − x, 3/2 − y, 3/2 − z) 2.310(3) Å, the sum of covalent radii of Hg atom being 2.96 Å[7]) lead to the suggestion that there are anionic chains $(Hg_3I_8^{2-})_n$ in the real structure where tetrahedra with Hg atom population equal to 1 alternate with tetrahedra in which Hg atom populations are vacant. Figure 1 shows that in the anionic chain on the c ~ 1/4 level the positions of Hg(1) with x = 0.5 and Hg(2) with x = 0.1565 and 0.8435 are vacant and in the chain of c ~ 3/4 level the positions of Hg(1) with x = 0 and Hg(2) with x = 0.3435 and 0.6565 are vacant.

Bond lengths and valency angles in the $Hg_3I_8^{2-}$ anion are given in Table II. Hg(1) atom has tetrahedral configuration of bonds with C_2 symmetry. Shortening of symmetrical bond lengths Hg(1)-I(1) and Hg(1)-I(1″) to 2.431(2) Å and increasing of the angle between these bonds to 151.5(2)° corresponds to the tendency of Hg(1) atom to diagonal coordination. Due to this tendency the bonds of Hg(1) atom with other iodine atoms are lengthened considerably: Hg(1)-I(2) and Hg(1)-I(2″) are equal to 3.391(3) Å.

Unlike Hg(1) atom tetrahedral configuration of Hg(2) atom bonds has no crystallographic symmetry and is less distorted: bond lengths Hg(2)-I vary in the range 2.552(3)–3.092(3)Å, and valency angles I-Hg(2)-I in the range of 99.9(2)–128.1(2)°. Two types of HgI_4 tetrahedra were found for $Cs_2Hg_3I_8.H_2O$[16,17] where the $Hg_3I_8^{2-}$ anion is described by layers of vertex-sharing HgI_4 tetrahedra.

In $(BEDT\text{-}TTF)_4Hg_3I_8$ structure shortened contacts between anionic and cationic sheets have not been discovered.

The conductivities of monocrystals along three dimensions were measured by standard four probe DC method. The contacts (10 μ diameter) were attached to the crystals with graphite paste. The conductivity measured at room temperature along the **b** axis for various monocrystals is in the range of (0.3–2) $(ohm.cm)^{-1}$. The conductivity measurements along the **a** axis and along the **b** axis show that the anisotropy in the crystal plane is absent, which is explained by the existence of shortened contacts between the cationic stacks. It should be noted that there are no shortened contacts between the molecules inside the stacks. The conductivity measured in the transverse direction (two contacts attached to one crystal plane, the other two to an opposite one) corresponds to the anisotropy of ca. 10^3.

The temperature dependence of the $(BEDT\text{-}TTF)_4Hg_3I_8$ monocrystal conductivity along the **b** axis is given in Figure 3. As seen the plane phase transition semiconductor-dielectric occurs in the salt at T = 260 K. At this temperature, the

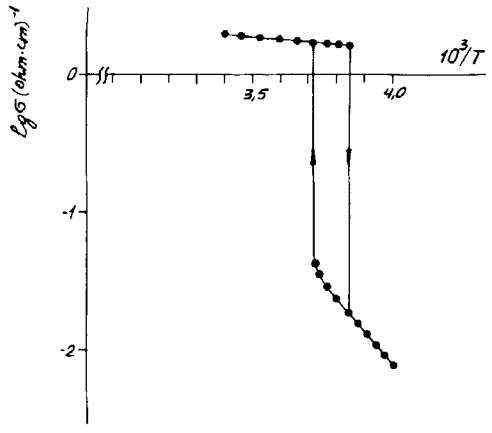

FIGURE 3 The temperature dependence of the conductivity showing the first order phase transition in this region.

conductivity sharply decreases by 1–1.5 orders of magnitude. The activation energy above the transition is $E_1 = 500$ K and below it $E_2 = 5500$ K. The presence of hysteresis of ~8 K wide occurs in the transition from one phase to another, which is indicative of the first type structural phase transition. The structural transition of a similar type was observed for the $MEM(TCNQ)_2$ anion-radical salt.[18] It may be assumed (however, with small probability) that the ambiguity of mercury atoms positions in the anion layer disappears in the transition to the new phase.

When cycling the temperature near the transition point (±20 K) the conduction course registered in the crystal plane is not reproduced: at temperatures below transition it always remains activated although the gap width may change. At temperatures above the transition the conductivity character can qualitatively change from semiconductive to metallic. For some BEDT-TTF salts,[19] particularly for those with chlorinemercurate anion[20] there is known a significant dependence of conductivity on pressure. In the process of cycling near the phase transition there is a possibility of appearance of some random domains with internal stress. This may be probably result in conductivity spread for different cycles, and even metallization, in the high-temperature phase. The temperature dependence of the conductivity of $(BEDT\text{-}TTF)_4Hg_3I_8$ at a hydrostatic pressure of $P = 29$ kbar shows (Figure 4) the phase transition observed at atmospheric pressure to disappear completely, the resistivity down to 50 K to decrease by ca. 10%, then, approaching helium temperature, to increase four times.

It is worth mentioning that the temperature dependence measured in transverse direction coincides with similar measurements in the crystal plane. However, at multiple cycling, the value of the previous cycle is reproduced with an accuracy of 2–3%. It is naturally assumed that during phase transition the significant changes take place in the cationic or anionic sheets, the situation between the layers remaining the same.

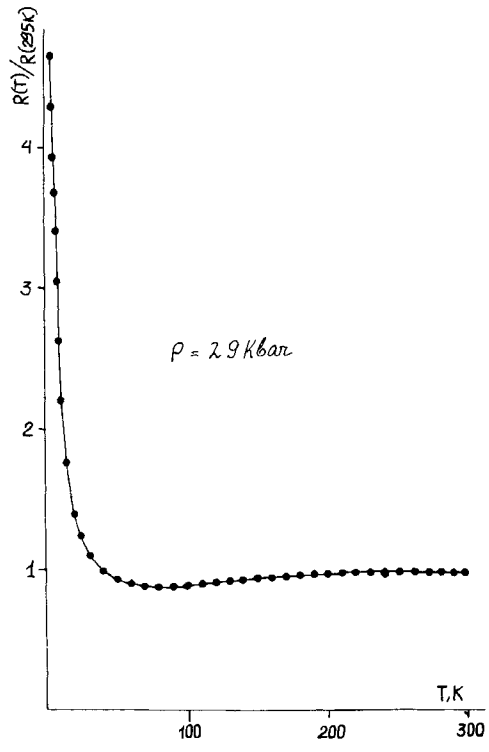

FIGURE 4 The temperature dependence of the resistivity for the single crystal at high pressure.

The temperature dependence of thermopower is shown in Figure 5. At high temperatures it does not depend on temperature (S (300 K) = +55 μV/K) and on lowering the temperature down to T = 260 K it has a break followed by a hysteresis cycle of ~8 K. Right after the transition, the thermopower decreases down to zero and then sharply increases with a negative sign at a temperature decrease. The temperature independence of thermopower and its magnitude mean that it is the spin entropy that makes the main contribution to thermopower as is characteristic of TCNQ salts[21] with strong Coulomb electron repulsion at one site.

Thermopower below phase transition is changed by $\sim T^{-1}$ and described by a formula applicable for semiconductors

$$S = -\frac{k}{e}\left(\frac{E_a}{kT} + A\right)$$

Here, the activation energy corresponds to E_a = 6000 K. This value correlates well with the activation energy of the conductivity below transition temperature.

Figure 6 shows the temperature dependence of the static paramagnetic susceptibility of $(BEDT\text{-}TTF)_4Hg_3I_8$. At high temperatures ($T > 50$ K) the χ_p behavior is described by the Curie (Weiss) law with the Curie constant approximately cor-

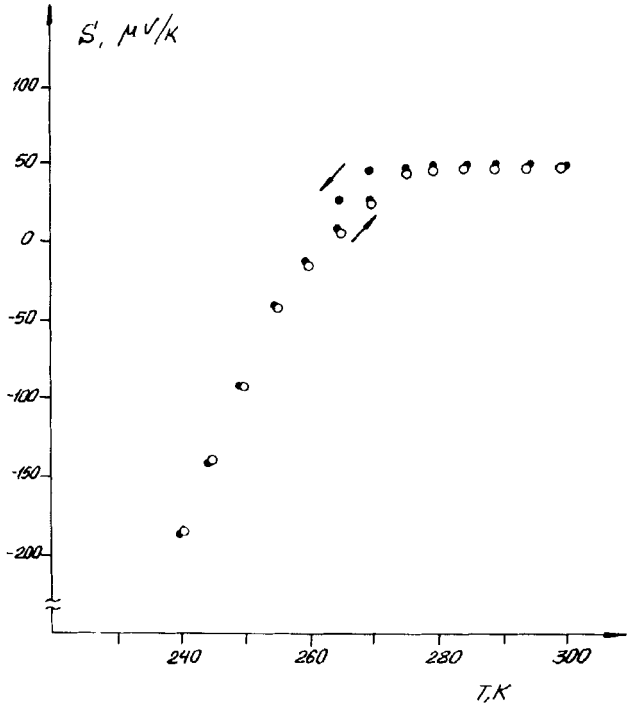

FIGURE 5 The thermopower along b axis vs. temperature.

responding to a localized electron per two molecules of BEDT-TTF. Such a behavior corresponds to the stoichiometric formula of the compound according to which an average BEDT-TTF charge is +0.5. The implementation of the Curie law in χ_p corresponds to the thermopower behavior (at high temperatures) which suggests that the electrons are localized on the BEDT-TTF molecules because of strong Coulomb repulsion. At the phase transition temperature, $T \approx 260$ K, in the region with the most marked jumps in conductivity and thermopower, the χ_p behavior is not very peculiar. The low-temperature behavior of χ_p is described by the formula

$$\chi_p = \frac{N\mu_B^2 g^2}{KT} (3 + \exp(2J/KT)^{-1}$$

(where $2J = 55$ K) typical for a system of isolated paired sites. Here J is the exchange energy inside the pair. According to the X-ray structural data, at high temperatures the BEDT-TTF molecules are coupled in pairs interconnected by shortened intermolecular contacts, while the neighboring pairs are interconnected weaker. In terms of magnetic properties, these pairs are thought to be isolated sites containing one electron each and interconnected into a two-dimensional network in the **ab** plane. At phase transition this network is assumed to undergo

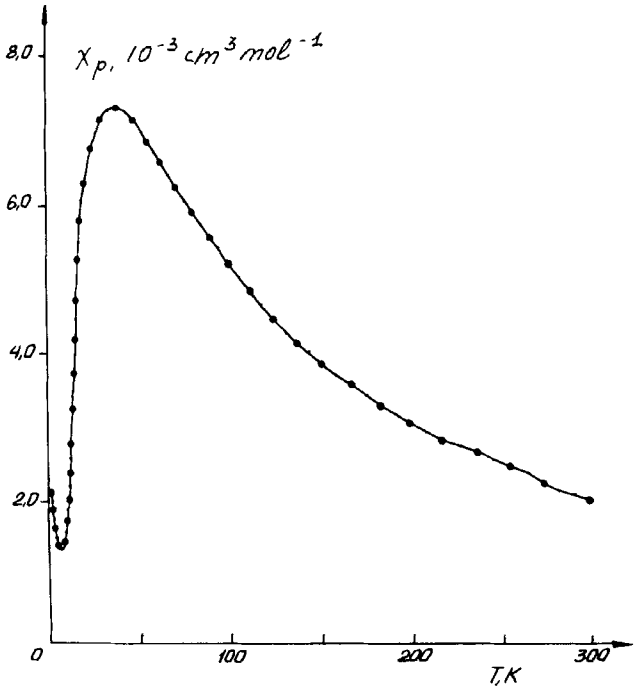

FIGURE 6 The temperature dependence of the static paramagnetic susceptibility of (BEDT-TTF)$_4$Hg$_3$I$_8$.

alternation so that these sites are coupled into pairs, more or less isolated from each other.

References

1. E. B. Yagubskii, I. F. Shchegolev, V. B. Laukhin, P. A. Kononovich, A. V. Zvarykina and L. I. Buravov, *Pis'ma v Zh. Eksp. Teor. Fiz.*, **39**, 12 (1984).
2. R. Kato, H. Kobayashi, S. Moriyama, Y. Nishio, K. Kajita and W. Sasaki, *Chem. Lett.*, 507 (1987).
3. J. M. Williams, H. H. Wang, M. A. Beno, T. J. Emge, L. N. Sowa, P. T. Copps, F. Behroczi, L. N. Hall, K. D. Carlson and G. N. Crabtree, *Inorg. Chem.*, **23**, 3839 (1984).
4. E. Amberger, H. Fuehs, K. Polborn, *Angew. Chem. Intern. Ed. Engl.*, **24**, 1968 (1985).
5. H. Urayama, H. Yamochi, G. Saito, A. Kawamoto, J. Tanaka, T. Mori, Y. Mariyama and H. Inokuchi, *Chem. Lett.*, 463 (1988).
6. S. S. P. Parkin, E. E. Engler, R. R. Shumaker, R. Lagier, V. Y. Lee, G. C. Scott and R. L. Greene, *Phys. Rev. Lett.*, **50**, 270 (1983).
7. D. Grdemie, *Quart. Rev.*, **19**, 303 (1965).
8. T. Robinson, *Int. Congr.*, **A43**, C1–C360 (1987).
9. R. N. Lyubovskaya, R. B. Lyubovskii, R. P. Shibaeva, M. Z. Aldoshina, L. M. Goldenberg, R. B. Rozenberg, M. L. Khidekel and Yu. F. Shulpyakov, *Pis'ma v Zh. Eksp. Teor. Fiz.*, **42**, 380 (1985).
10. R. N. Lyubovskaya, E. I. Zhilyaeva, S. I. Pesotsky, R. B. Lyubovskii, L. O. Atovmyan, O. A. Dyachenko and T. G. Takhirov, *Pis'ma v Zh. Eksp. Teor. Fiz.*, **46**, 149 (1987).
11. J. B. Dearon and B. O. West, *J. Chem. Soc.*, 3929 (1961).
12. V. I. Andrianov, Z. Sh. Safina and B. L. Tarnopolskii. "Reuntgen-75". An Automatic System of Programs for Crystal Structure Solution (Russ.), Chernogolovka, 1975.

13. T. V. Timofeeva, N. Yu. Chernikova and P. M. Zorky, *Usp. Khim.*, **49**, 966 (1980).
14. H. Kobayashi, *Chem. Lett.*, 183 (1984).
15. V. E. Korotkov, N. D. Kushch, M. K. Makova, R. P. Shibaeva and E. B. Yagubskii, *Izvestija AN SSSR, ser khim*, **N7**, 1686 (1988).
16. P. M. Fedorov and V. I. Pakhomov, *Koord. Khim.*, **1**, 670 (1975).
17. R. Sjövall and C. Svensson, *Acta Cryst.*, **C44**, 207 (1988).
18. R. C. Lacoe, G. Gruner and P. M. Chaikin, *Solid State Comm.*, **36**, 599 (1980).
19. M. V. Kartsovnic, P. A. Kononovich, V. N. Laukhin, A. G. Khomenko and I. F. Shchegolev, *Zh. Eksp. Teor. Fiz.*, **88**, 12 (1984).
20. R. B. Lyubovskii, N. V. Kapustin and R. N. Lyubovskaya, *Zh. Eksp. Teor. Fiz.*, **93**, 1863 (1987).
21. R. Somoano, V. Hadek, S. P. Yen, A. Rembaum and R. Deck, *J. Chem. Phys.*, **62**, 1061 (1975).